

Sensorless speed control of DC motor using EKF estimator and TSK fuzzy logic controller

Ravi Pratap Tripathi, Ashutosh Kumar Singh, Pavan Gangwar & Ramesh Kumar Verma

To cite this article: Ravi Pratap Tripathi, Ashutosh Kumar Singh, Pavan Gangwar & Ramesh Kumar Verma (2022) Sensorless speed control of DC motor using EKF estimator and TSK fuzzy logic controller, *Automatika*, 63:2, 338-348, DOI: [10.1080/00051144.2022.2039990](https://doi.org/10.1080/00051144.2022.2039990)

To link to this article: <https://doi.org/10.1080/00051144.2022.2039990>



© 2022 The Author(s). Published by Informa UK Limited, trading as Taylor & Francis Group



Published online: 21 Feb 2022.



Submit your article to this journal [↗](#)



Article views: 1171



View related articles [↗](#)



View Crossmark data [↗](#)



Sensorless speed control of DC motor using EKF estimator and TSK fuzzy logic controller

Ravi Pratap Tripathi ^a, Ashutosh Kumar Singh ^a, Pavan Gangwar ^a and Ramesh Kumar Verma^b

^aDepartment of Electronics and Communication Engineering, Indian Institute of Information Technology Allahabad, Prayagraj, India;

^bDepartment of Electronics and Communication Engineering, Bundelkhand Institute of Engineering & Technology, Jhansi, India

ABSTRACT

In this article, sensorless speed control of DC motor has been proposed using the extended Kalman filter (EKF) estimator and Takagi–Sugeno–Kang (TSK) fuzzy logic controller (FLC). In the industry, high-cost measurement systems/sensors are necessary for better controlling and monitoring, which can be replaced by a sensorless control technique to reduce the cost, size and increase system reliability and robustness. EKF has been used to perform the sensorless speed control by estimating the speed of the DC motor using the armature current only and TSK-FLC is used to reduce the effect of motor parameter variation and load torque nonlinearity in close loop speed control for various speed references. The performance of EKF-based TSK-FLC is compared with EKF-based PID controller. The time-domain specification and absolute error performance indices indicate that EKF-based TSK-FLC is superior to the EKF-based PID under similar conditions. The proposed system is executed in the MATLAB/Simulink environment, and sensorless speed control of DC motor prototype model has been developed for validating the proposed technique with the help of a micro-controller.

ARTICLE HISTORY

Received 5 September 2021
Accepted 4 February 2022

KEYWORDS

Extended Kalman filter;
sensorless speed control;
fuzzy logic controller; DC
motor; MATLAB

1. Introduction

DC motor drives are widely used electrical machines in many applications, including rolling factories, paper mills, robots, electrical vehicles and others for which adjustable speed and constant or low-speed torque are required. Nowadays, there exist a wide variety of schemes to control the speed of electrical machines [1]. A PID controller has been implemented on LabVIEW and motor speed is measured by a sensor [2], whereas various optimization algorithms to tune the PID parameters have been discussed in [3]. The PW (pulse width modulation) controlled BLDC motor drives have been discussed in [4,5]. Shanmugasundram et al. [6] investigated the performance of fuzzy and PID controller for BLDC servomotor; however, the speed of the motor was regulated by a PWM-controlled chopper driver. In the above techniques, researchers used a speed sensor or tachogenerator to measure the speed, which increases the hardware complexity and cost along with reduced reliability. To achieve effective speed control, a closed-loop speed control system with known or feedbacked motor state variables has been required. Therefore, to measure all the state variables of the system, various mechanical sensors are required which will not only increases the system size, complexity and overall cost but also minimize the robustness and reliability. To minimize the number of sensors and system complexity, the researchers focused on sensor-

less control strategy along with intelligent control for optimum response [7].

In sensorless control techniques, the speed of motor is estimated by an observer/estimator with the use of relevant electrical signals [8]. Sliding mode observer [9–11], model reference adaptive system [12–14], Luenberger observer [15], Kalman filter (KF) [16] and extended Kalman filter (EKF) [17–20] are widely used state estimation techniques. The observer uses some mathematical equation with some measured states (current, voltage) of a motor to estimate the speed/position. An ANN-based sensorless speed control technique of DC motor has been discussed [21]. In [22], improved speed estimation performance of PMSM drive has been obtained by replacing the saliency back EMF estimator using the PID to a PID neural network torque observer. Cao et al. [23] implemented a low-speed control strategy of PMSM drive, using an adaptive Kalman filter (AKF), incremental encoder and PI control. Some sensorless speed estimation techniques have been discussed with the fuzzy logic controller (FLC) for the BLDC motor [24–27]. The speed of the induction motor is controlled by a Luenberger observer with Fuzzy-PID [28,29]. Al Maliki and Iqbal [30] implemented an FLC-based sensorless speed control technique for DC motor utilizing KF observer. KF is a linear time state estimator which is widely used for linear and known system parameters,

but in practical application, the system is nonlinear. So the performance of KF starts degrading. To overcome the nonlinearity problem, EKF is a widely used state estimator.

The performance of sensorless speed control directly depends on the performance of the estimation algorithm. To design a good sensorless speed controller, it is essential to know the exact mathematical model of motor and environmental disturbance; but in practical applications, generally, systems are found nonlinear, complex, environmental disturbances are uncertain and it is generally assumed that motor parameters never change. However, in practical application load parameters, inertia, friction, temperature and reference speed change create problems for optimum response.

In this paper, TSK-FLC with an EKF has been used to achieve optimum response and better speed tracking irrespective of change in reference speed, motor parameter variation and load torque (constant or nonlinear). In this technique, DC motor shaft speed has been estimated by EKF observer with the help of sensed armature current only. The estimated shaft speed is feedbacked to the TSK-FLC for generating a control signal to perform the closed-loop speed sensorless control of the DC motor. The organization of the paper is: In Section 2, a DC motor mathematical model has been presented. EKF state estimation algorithm is presented in Section 3, while the implementation of EKF with TSK-FLC is discussed in Section 4. Results and concluding remarks are presented in Sections 5 and 6, respectively.

2. DC motor mathematical model

State estimation algorithm for a DC motor requires a mathematical model in the time domain. The mathematical model of the DC motor has two main equations, one is electrical and the other one is mechanical [31]. By applying Kirchhoff's second law in armature circuit presented in Figure 1, the electrical equation is given as

$$v(t) = e_a(t) + R_a i_a(t) + L_a \frac{d}{dt} i_a(t) \quad (1)$$

where i_a is armature current, R_a is the armature resistance, L_a is the armature self-inductance caused by armature flux, v_t is armature supply voltage and $e_a(t)$ is back emf. A separately excited DC motor presented in Figure 1 requires an extra DC voltage (u_f) to produce the magnetic field. L_f and R_f represent the inductance and resistance of the field winding, respectively. It is well known that when the field voltage constant and steady-state exists in the field circuit, then i_f is constant therefore Equation (1) can be written as

$$v(t) = K'_e \omega_m(t) + R_a i_a(t) + L_a \frac{d}{dt} i_a(t) \quad (2)$$

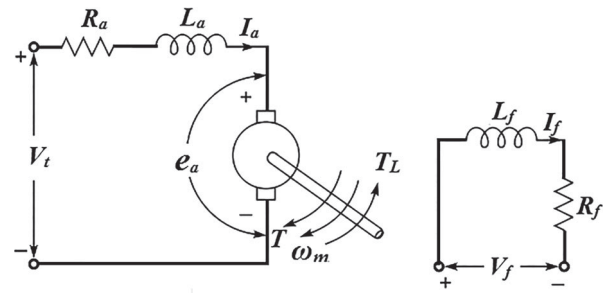


Figure 1. Schematic of separately excited DC motor.

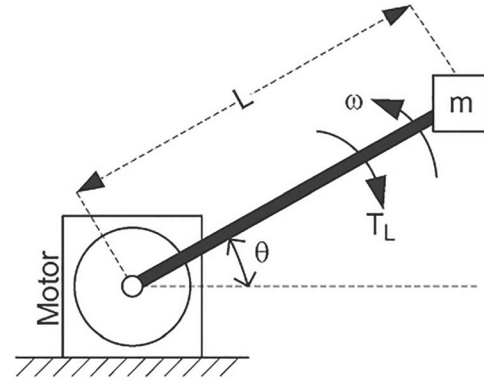


Figure 2. Nonlinear load model for DC machine.

For motoring operation, the dynamic equation for the mechanical system is

$$T(t) = K_t i_f(t) i_a(t) = J \frac{d}{dt} \omega_m(t) + T_L(t) + T_f(t) + D \omega_m(t) \quad (3)$$

where ω_m is the motor speed, J moment of inertia of motor and load, D is viscous damping coefficient, $T_f(t)$ is coulomb friction torque and T_L is load torque as shown in Figure 2, can be expressed as

$$T_L = mgL \cos \theta + mL^2 \frac{d}{dt} \omega_m(t) \quad (4)$$

where m represents the mass of load, L is arm's length, g is gravitational constant and θ is angular displacement, integral of ω_m . The details of motor parameters are given in Appendix. The Simulink model of the load model is given in Figure 3.

As i_f is constant then Equation (3) can be written as

$$T(t) = K'_t i_a(t) = J \frac{d}{dt} \omega_m(t) + T_L(t) + T_f(t) + D \omega_m(t) \quad (5)$$

With the help of Equations (2) and (5), the state-space model can be implemented. The model comprises two state variables i.e. armature current (i_a) and motor speed (ω_m). The state-space model in the time domain is given as

$$\begin{bmatrix} \dot{\omega}_m \\ \dot{i}_a \end{bmatrix} = \begin{bmatrix} \frac{D}{mL^2+J} & \frac{K'_t}{mL^2+J} \\ \frac{-K'_t}{L_a} & \frac{-R_a}{L_a} \end{bmatrix} \begin{bmatrix} \omega_m \\ i_a \end{bmatrix}$$

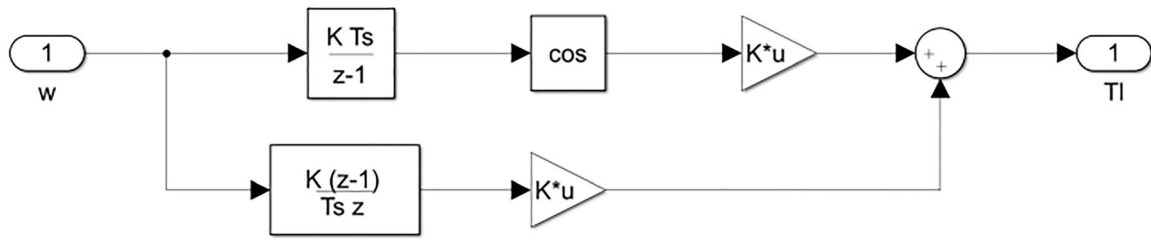


Figure 3. Simulink model of load.

$$+ \begin{bmatrix} \frac{mgL \cos \theta - T_f}{mL^2 + J} & 0 \\ 0 & \frac{-R_a}{L_a} \end{bmatrix} \begin{bmatrix} 1 \\ v_t \end{bmatrix} \quad (6)$$

From the state-space model, it is clear that θ produces nonlinearity in the system. For digital implementation, Equation (6) must be discretized. The discrete-time model of the system can be represented in the form of the following equations:

$$x_{k+1} = A_d x_k + B_d u_k + v_k \quad (7)$$

$$y_k = C_d x_k + w_k \quad (8)$$

In the above equation, x (state variable) = $[\omega_m, i_a]^t$, u (input vector) = $[1, v_t]^t$, y (output vector) = $[0, i_a]^t$, v and w is the process noise and measurement noise with covariance Q and R , respectively, at mean zero. At sampling interval T_s , the discretized matrix coefficients A_d , B_d and C_d can be written as

$$A_d = I + AT_s = \begin{bmatrix} 1 & 0.005 \\ -0.007 & 0.9828 \end{bmatrix} \quad (9)$$

$$B_d = BT_s = \begin{bmatrix} -0.016 & 0 \\ 0 & 0.0067 \end{bmatrix} \quad (10)$$

$$C_d = C = [0 \quad 1] \quad (11)$$

With the help of Kalman controllability and observability test, we find that the above system is controllable and observable, which implies that we can design a controller and observer. The detail of the EKF estimator/observer and their performance has been presented in the next section.

3. EKF observer

The observer uses the state-space model generated in Section 2 to estimate the motor speed (ω_m) based on i_a measurements. KF is a state observer that computes the best feasible state from a noisy state using iterative mathematical equations. For nonlinear systems, the KF is not relevant in the presented system as the load torque is nonlinear (in the calculation of θ using ω_m leads the DC motor model to nonlinear). Therefore, EKF is used to overcome the nonlinear difficulty of KF. EKF is the extended version of KF which uses first-order Taylor series approximation of nonlinear dynamical function to estimate the state by noisy measured data. The EKF

has two main steps: one is state prediction and the other is state correction. In the prediction step, a dynamical model of the system with process noise covariance Q is used. In the correction step, the predicted state is corrected with the help of measured data and Kalman gain (K). However, in the application of EKF, initial values of all the covariance matrices Q , R and P must be tuned correctly otherwise the system may become unstable and can diverge. The covariance can be achieved by analyzing the stochastic characteristics of the corresponding noise. Here, these are obtained intuitively and with the help of [17]. The EKF mathematical steps are presented below.

The prediction step is

$$\hat{x}_{k+1/k} = f(\hat{x}_k, u_k) \quad (12)$$

$$P_{k+1/k} = A_d P_k A_d' + Q \quad (13)$$

where \hat{x}_k represents the estimated state of x_k . The correction step is

$$K_{k+1} = P_{k+1/k} C_d' (C_d P_{k+1/k} C_d' + R)^{-1} \quad (14)$$

$$\hat{x}_{k+1} = \hat{x}_{k+1/k} + K_{k+1} (y_{k+1} - C_d \hat{x}_{k+1/k}) \quad (15)$$

$$P_{k+1} = P_{k+1/k} (I - K_{k+1} C_d) \quad (16)$$

where K_{k+1} is Kalman gain at $k+1$ time indices and I is the identity matrix. From Equations (12)–(16) is one complete cycle of the EKF algorithm.

4. Design and implementation of proposed model

The block diagram and MATLAB/Simulink model of the proposed system are shown in Figures 4 and 5, respectively. It consists of two blocks, one is the controller block and the other one is the DC motor block. In the controller block, TSK-FLC, EKF observer and PWM generators are present. In the EKF estimator block, EKF code has been written using the MATLAB code generator block to estimate the states (speed and current) of the DC motor. The difference between reference speed and estimated speed generates the error signal. The generated error and change in error are applied as an input to the fuzzy controller, which generates the duty cycle to produce the pulse width to control the speed of the DC motor. The TSK-FLC as represented in Figure 6 is an intelligent controller

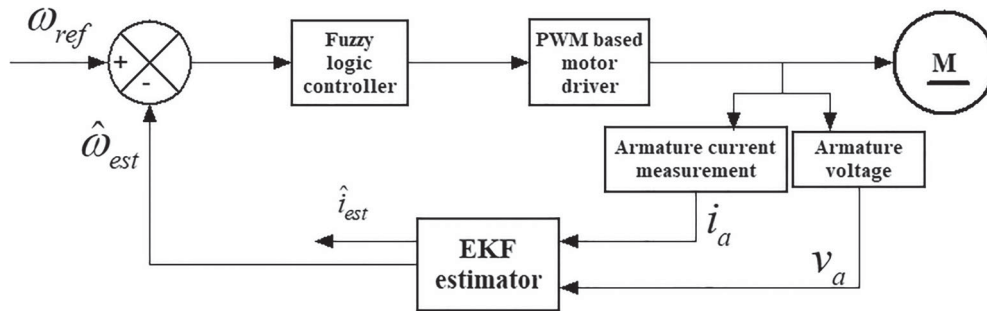


Figure 4. Block diagram of the proposed system.

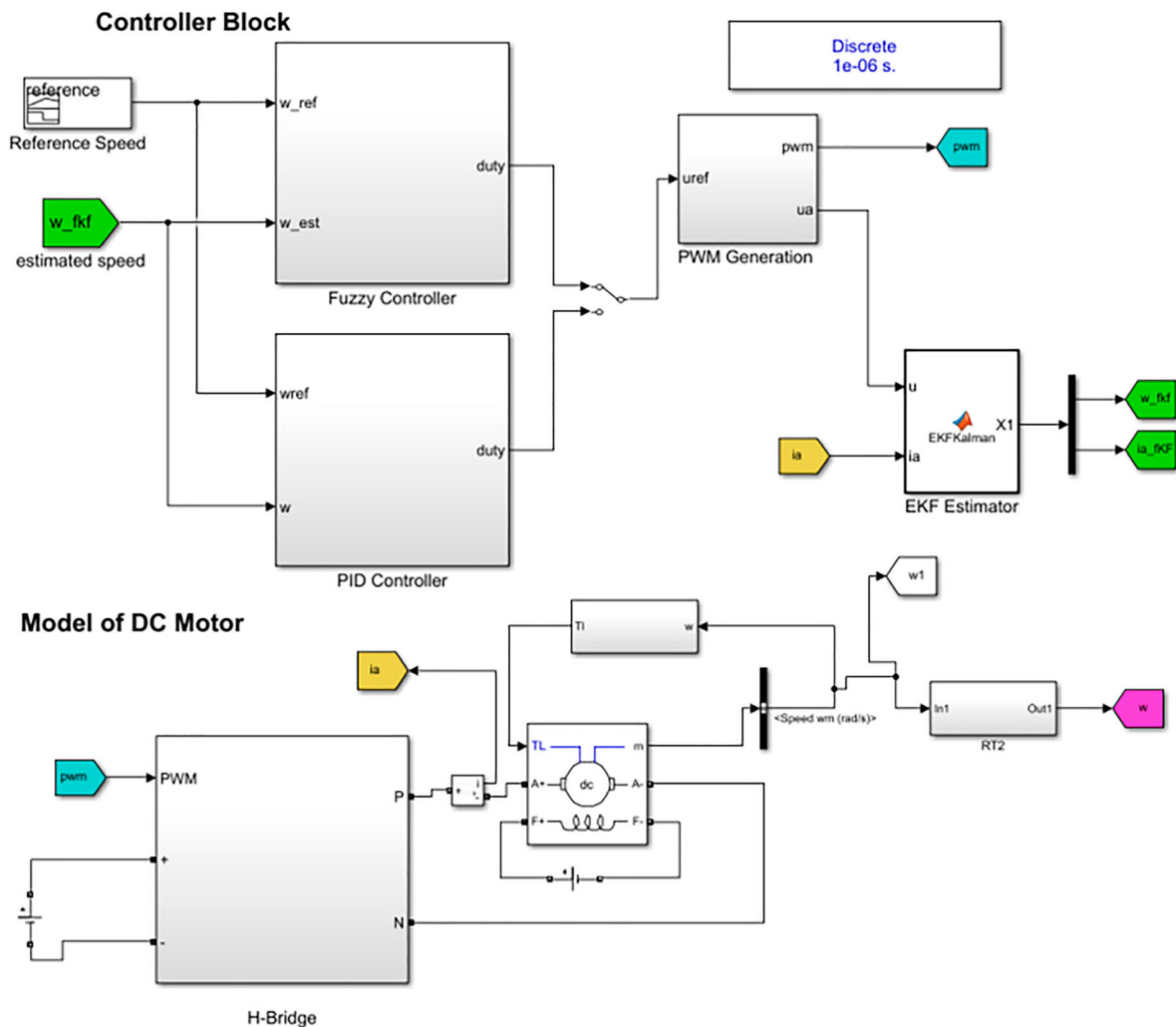


Figure 5. Simulink model of the proposed system.

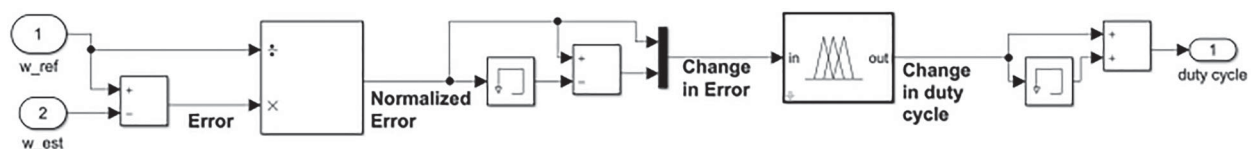


Figure 6. Simulink model of fuzzy controller.

to control complex and nonlinear systems. The FLC seems an ultimate solution in terms of high dynamic response and best disturbance rejection. The special merit of this controller is that it does not require the knowledge of a mathematical model of the plant for

the adaptation mechanism, and it can be easily implemented. It allows the designer to present the overall system behaviour linguistically by establishing rules in the form of IF-THEN statements. The general FLC structure has four parts: fuzzification, fuzzy rule base, fuzzy

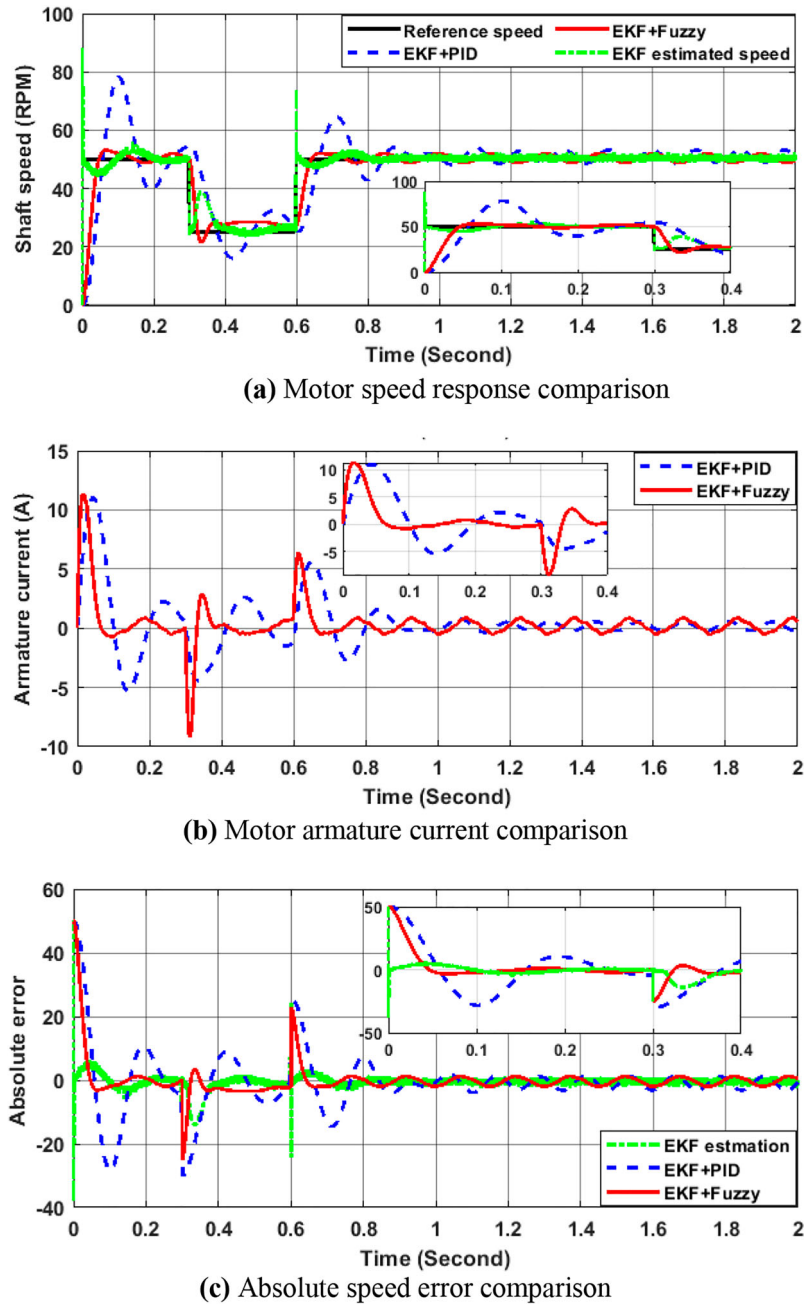


Figure 7. Simulation results at variable reference speed and nonlinear load ($T_L = mgL \cos \theta + mL^2 \frac{d}{dt} \omega_m(t)$).

inference and last is defuzzification, but TSK-FLC does not have a defuzzification stage. In TSK-FLC, the crisp result is obtained using the weighted average of rules, which makes it computationally efficient and more flexible in controller designing. In the fuzzification process, crisp (real) value is converted into linguistic (fuzzy) value. In the proposed technique, normalized error ($e = \omega_{ref} - \omega_{est}$) and change in error ($\Delta e = e_k - e_{k-1}$) are the fuzzified inputs. Three fuzzy variables are used for error {Negative, Zero, Positive} and three fuzzy variables {Negative, Zero, Positive} are used for change in error. In the proposed technique, triangular membership function has been used and fuzzy inference system rules are given in Table 1. Each rule takes two inputs, errors and changes in error to produce a corresponding change in duty cycle (ΔD). So the new duty cycle

Table 1. Fuzzy rule base.

Change in duty cycle		Error		
		Negative	Zero	Positive
Change in error	Negative	D	D	I
	Zero	D	Z	I
	Positive	D	I	I

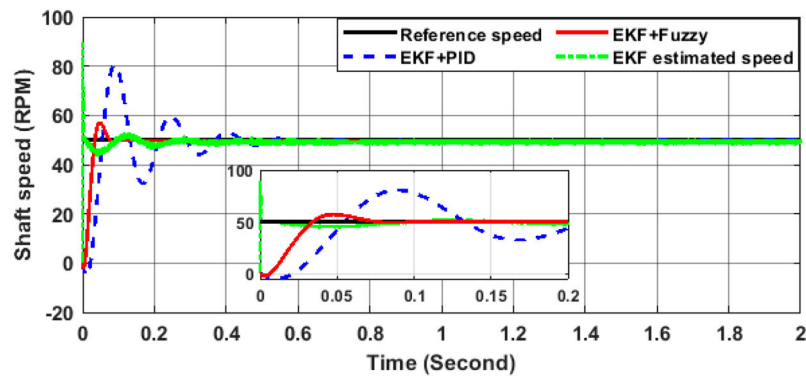
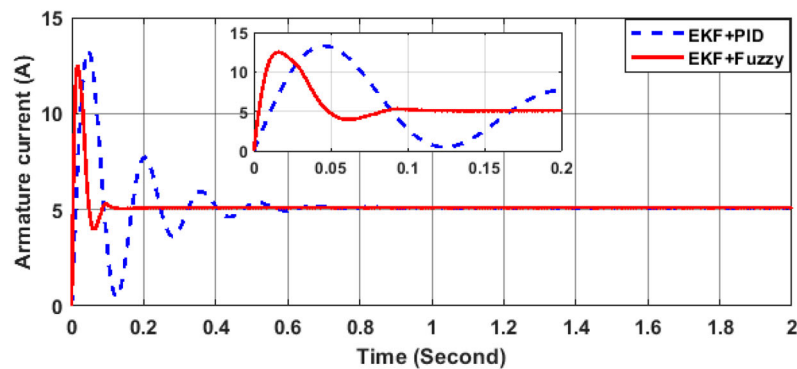
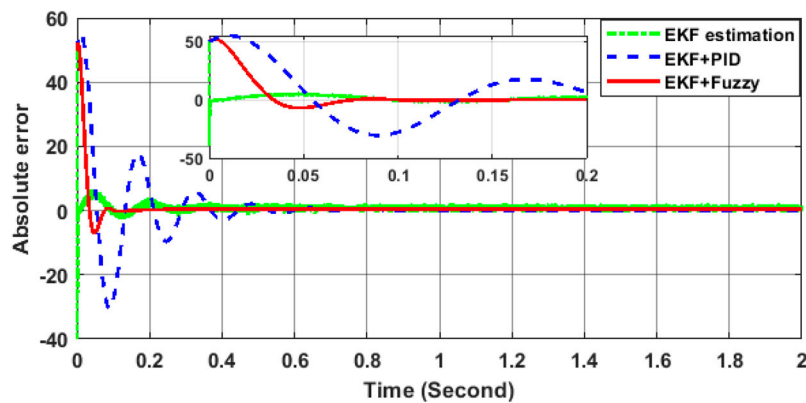
(D_{new}) of PWM signal for the motor driver is given as

$$D_{new} = D_{Previous} + \Delta D \quad (17)$$

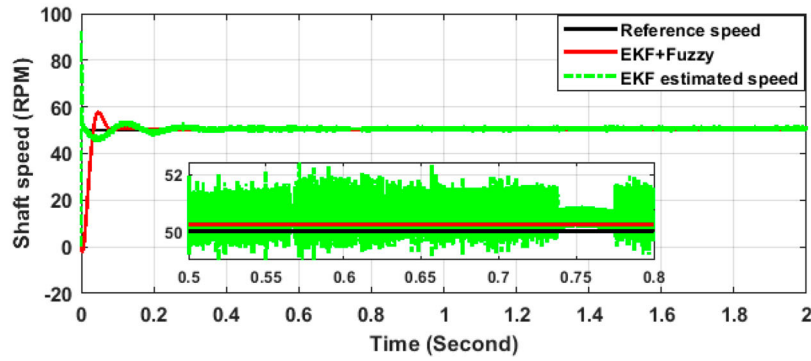
To implement the EKF with FLC-based sensorless speed control, the following steps are involved:

Table 2. Transient response comparison.

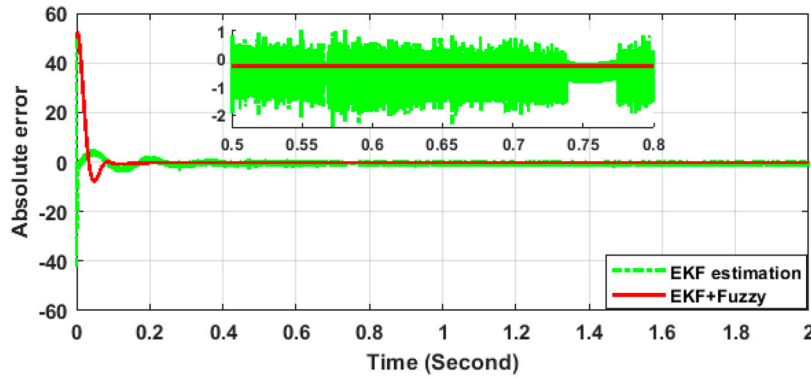
Controller	Rise time (s)	Overshoot (%)	Settling time (s)	Average absolute error
EKF with PID	0.0558	35	0.5	4.57
EKF with TSK-FLC	0.03543	17	0.18	1.5

**(a)** Motor speed response comparison**(b)** Motor armature current comparison**(c)** Absolute speed error comparison**Figure 8.** Simulation results of EKF with PID and EKF with fuzzy at constant load and reference speed 50 rpm.

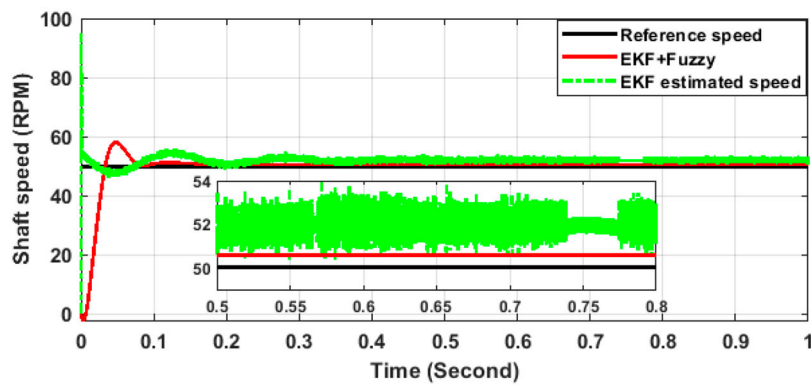
- (1) Assign the initial values of states (motor speed, armature current) and the values of error covariance P , Q and R .
- (2) Predict the next states (motor speed) with the help of Equations (12) and (13).
- (3) Measure the armature current with the help of the current sensor and correct the predicted state with the help of Equations (14) and (15). This corrected state is used as the previous state for state prediction in the next iteration.
- (4) Compare the corrected speed (ω_{est}) with the reference speed (ω_{ref}) and generate the error signal.
- (5) Now apply the generated error signal to the TSK-FLC to generate the appropriate PWM signal.
- (6) This PWM signal generates the corresponding voltage using an H bridge to drive the motor.



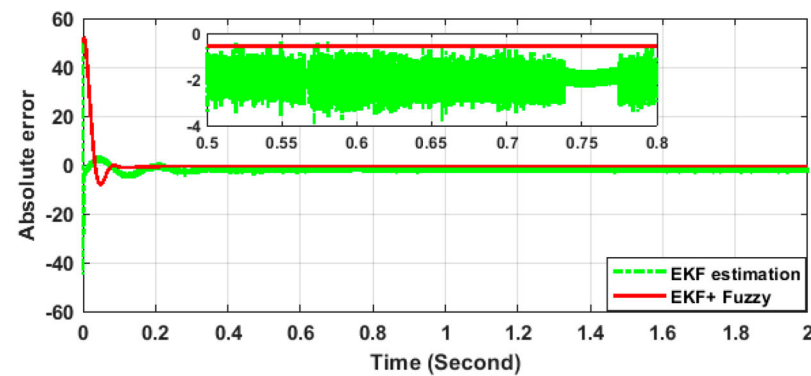
(a) Closed-loop speed response using EKF with fuzzy and EKF speed estimation at 25 °C



(b) Absolute error at 25 °C

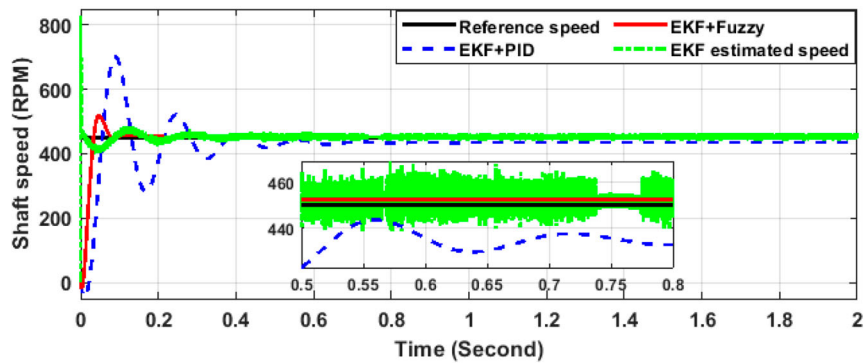


(c) Closed-loop speed response using EKF with Fuzzy and EKF speed estimation at 70°C

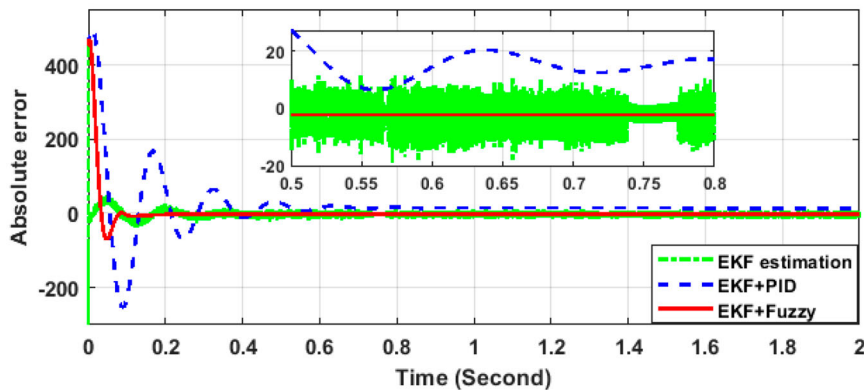


(d) Absolute error at 70 °C

Figure 9. Parametric variation simulation result of EKF with FLC at 25°C ($R_a = 2.581\Omega$) and 70°C ($R_a = 3.045\Omega$).



(a) Motor speed response comparison



(b) Absolute speed error comparison

Figure 10. Simulation results of EKF with PID and EKF with fuzzy at constant load and reference speed 450 rpm.

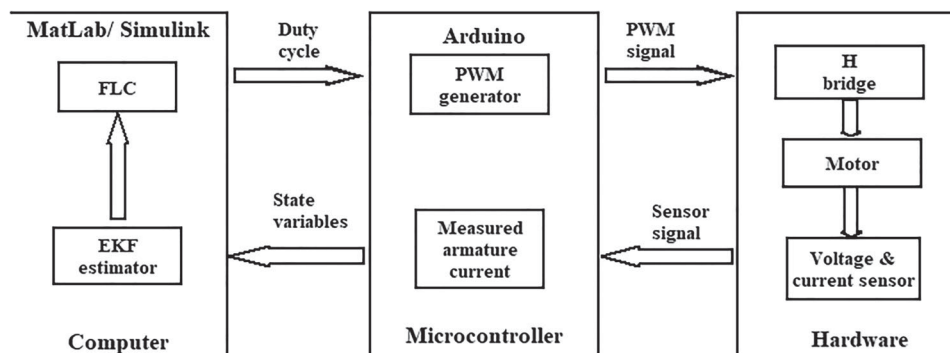


Figure 11. Block diagram of hardware in loop system design.

- (7) Repeat step-2 to step-6 for closed-loop speed control of the DC motor.

5. Results discussion and experimental validation

5.1. Simulated result

Sensorless closed-loop speed control of the DC motor is presented using an EKF with FLC. The closed-loop speed control performance of the EKF with PID and EKF with TSK-FLC at nonlinear load is shown in Figure 7(a). In Figure 7(b), the DC motor armature current of EKF with PID and EKF with TSK-FLC has shown. The absolute speed errors of EKF with PID and EKF with FLC, and speed estimation error are shown in Figure 7(c). The absolute speed errors are defined as

the Euclidean distance between reference speed and the corresponding real speed obtained by the corresponding controller. In Figure 7, the motor reference speed and load torque both are variable with time. From Figure 7(a), it can be analyzed that EKF estimates the motor speed very quickly without using any speed sensor. It also concludes that the EKF with FLC controller has better reference speed tracking capability in comparison with the EKF with PID controller. The time-domain specifications comparisons for both controllers are shown in Table 2.

To check the robustness of the EKF-based sensorless TSK fuzzy controller, a constant load of 20 Nm is applied at a constant reference speed of 50 rad/sec. The performance results at constant load are shown in Figure 8. In Figure 8(a), sensorless closed-loop speed

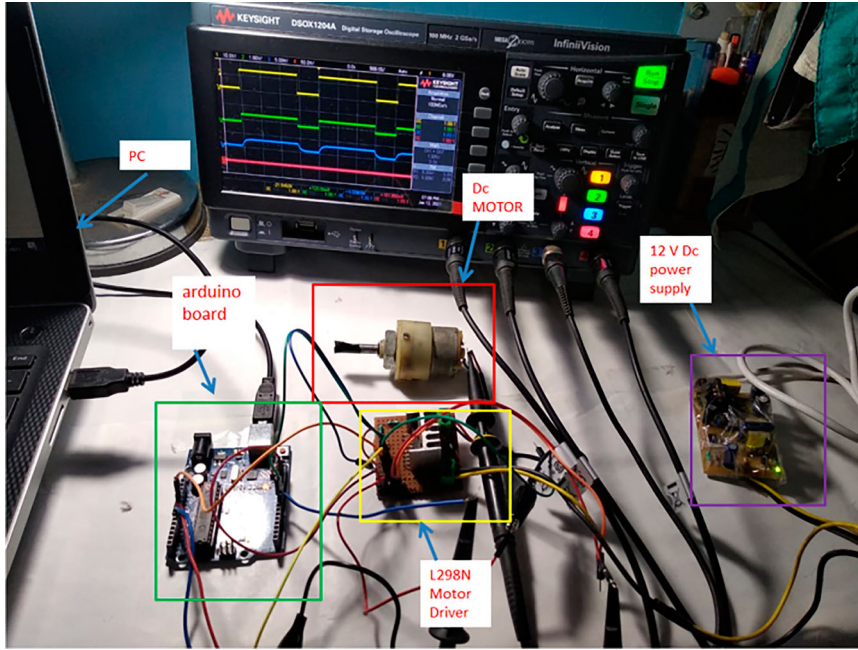
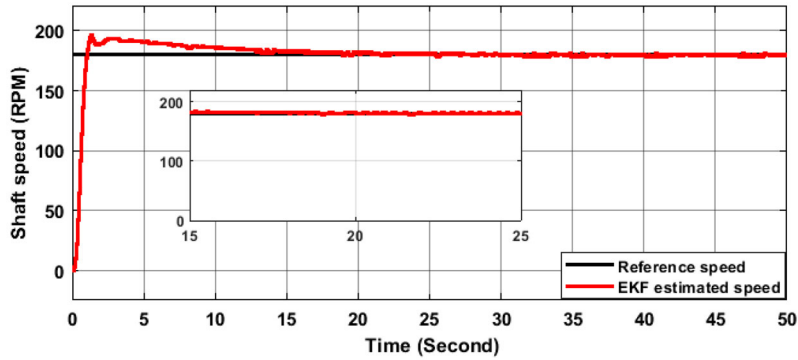
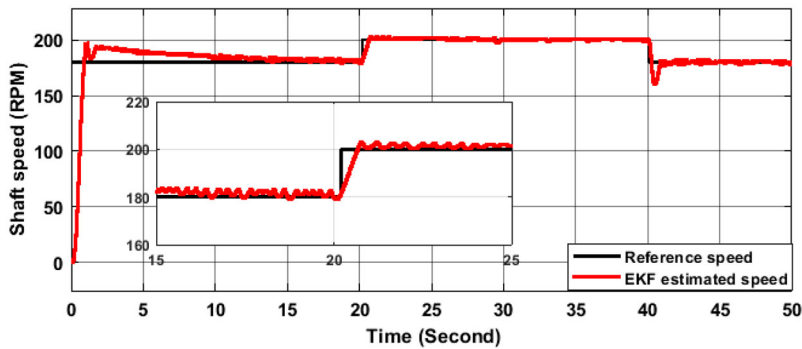


Figure 12. Experimental setup of sensorless speed control of DC motor.



(a) Experimental result at constant speed



(b) Experimental result at variable speed

Figure 13. Experimental prototype result validation at a constant speed and variable speed.

control performance using EKF with PID and EKF with TSK-FLC is shown. In the perusal of the figure, it can be observed that EKF with TSK-FLC has better reference speed tracking capability at constant load also. Figure 8(b, c) shows the comparison of armature current and absolute speed error performance at a constant speed and constant load, respectively.

In practical applications, the system parameters are not known accurately. Therefore, 5% differences are

considered in the real system model and filter parameter respectively. In Figures 7 and 8, the effect of change in load torque at various reference speeds is presented. In Figure 9 the effect of motor parameter variation is presented. It is well known, the resistance of motor armature depends on the temperature of the motor coil. The resistance of armature is increased by approximately 16% on increasing the coil temperature by 40°C. The resistance of motor armature is manually increased

in the simulation model of motor to exhibit the effect of temperature. In this study, the parameters of FLC and EKF algorithm are not changed. The result presented in Figure 9 shows that EKF estimated speed changes slightly on changing the armature resistance but the closed-loop speed response remains the same, i.e. the closed-loop speed response using EKF with Fuzzy is not truly dependent on the armature resistance which is raised by the temperature of motor coil.

The closed-loop speed control performance of the EKF with PID and EKF with TSK-FLC at 450 rpm and constant load has been presented in Figure 10 without changing the controller and EKF parameters. The result shows that the EKF estimator tracks the reference speed with $\pm 3\%$ error and the closed speed control performance using EKF with TSK-FLC is also good but the closed speed control performance using EKF with PID exhibit a permanent residual error. All the result studies show that closed-loop speed sensorless control performance of EKF with TSK-FLC is better than EKF with PID in all the cases. The analysis shows that the EKF estimator performance and EKF with TSK-FLC performances at high speed are poor in comparison with low-speed applications. One can get better performance by adjusting the observer covariance matrix and optimizing the TSK-FLC parameters or by changing and increasing the membership shape and value, respectively.

5.2. Experimental setup

To validate the proposed model, hardware in loop (HIL) simulation has been carried out. Figures 11 and 12 represents the schematic diagram of the HIL simulation and its experimental setup, respectively. The experimental setup involves four main components. The 12 V DC motor with a voltage and current sensor (L298N) motor driver module, Arduino board, and personal computer (PC). In PC, TSK-FLC and EKF estimator are present. The voltage across the motor winding and armature current is sensed by voltage and current sensor. This sensed value has been used to estimate the speed of the motor in the next iteration by the EKF estimator. The difference between reference speed and estimated speed generates the error signal for the controller block. The controller block generates the appropriate duty cycle. This duty cycle is applied to PWM inbuilt Arduino board which generates the PWM signals for the motor driver to control the speed of DC motor. To validate the proposed technique, the result of an experimental prototype has been presented in Figure 13. From Figure 13, it can be observed that the tracking of the reference speed is impressive. In light of the discussion of the above results, it can be concluded that EKF with TSK-FLC has better time-domain performance and good reference speed tracking ability in any conditions in comparison with EKF with PID.

6. Conclusion

In this paper, EKF with TSK-FLC and EKF with PID have been implemented for sensorless speed control of the DC motor. The EKF is used for speed estimation and later estimated speed is used by the TSK fuzzy controller for closed-loop speed control. The performance of both the controller with the EKF observer is compared in similar conditions. The MATLAB/Simulink and hardware prototype result of EKF with TSK-FLC shows satisfactory performance compared to EKF with PID over a wide range of speed and torque changes. An important component of the proposed technique is the adaptability of TSK-FLC with an EKF estimator for sensorless speed control. It shows high robustness toward parameter variation, improves tracking accuracy, reduces absolute error and improves the transient state performances.

Disclosure statement

No potential conflict of interest was reported by the author(s).

ORCID

Ravi Pratap Tripathi  <http://orcid.org/0000-0002-9731-8634>

Ashutosh Kumar Singh  <http://orcid.org/0000-0001-6342-8918>

Pavan Gangwar  <http://orcid.org/0000-0001-8139-8951>

References

- [1] Swarnkar P, Jain SK, Nema RK. Adaptive control schemes for improving the control system dynamics: a review. *IETE Tech Rev.* 2014;31(1):17–33.
- [2] Huang G, Lee S. PC-based PID speed control in DC motor. 2008 International Conference on Audio, Language and Image Processing, pp. 400–407, 2008.
- [3] Purnama HS, Sutikno T, Alavandar S., et al. Intelligent control strategies for tuning PID of speed control of DC motor - a review. 2019 IEEE Conference on Energy Conversion (CENCON), pp.24–30, 2019.
- [4] Sathyan A, Milivojevic N, Lee Y, et al. An FPGA-based novel digital PWM controls scheme for BLDC motor drives. *IEEE Trans Ind Electron.* 2009;56(8):3040–3049.
- [5] Lai Y-S, Shyu F-S, Chang Y-H. Novel loss reduction pulse width modulation technique for brushless DC motor drives fed by MOSFET inverter. *IEEE Trans Power Electron.* 2004;19(6):1646–1652.
- [6] Shanmugasundram R, Zakariah KM, Yadaiah N. Implementation and performance analysis of digital controllers for brushless DC motor drives. *IEEE/ASME Trans Mechatron.* 2014;19(1):213–224.
- [7] Mohan H, Pathak MK, Dwivedi SK. Sensorless control of electric drives a technological review. *IETE Tech Rev.* 2020;37(5):504–528.
- [8] Wang Q, Wang S, Chen C. Review of sensorless control techniques for PMSM drives. *IEEE Trans Electr Electron Eng.* 2019;14(10):1543–1552.
- [9] Mohan Krishna S, Febin Daya JL. A modified disturbance rejection mechanism in sliding mode state observer for sensorless induction motor drive. *Arab J SciEng.* 2016;41:3571–3586.

- [10] Lasca C, Boldea I, Blaabjerg F. A class of speed sensorless sliding-mode observers for high-performance induction motor drives. *IEEE Trans Ind Electron.* 2009;56(9):3394–3403.
- [11] Gan M-G, Zhang M, Zheng C-Y, et al. An adaptive sliding mode observer over wide speed range for sensorless control of a brushless DC motor. *Control Eng Pract.* 2018;77:52–62.
- [12] Sun X, Zhang Y, Tian X, et al. Speed sensorless control for IPMSMs using a modified MRAS with grey wolf optimization algorithm. *IEEE Trans Transp Electrification.* 2021: doi:10.1109/TTE.2021.3093580.
- [13] Dybkowski M, Orłowska-Kowalska T, Tarchała G. Sensorless traction drive system with sliding mode and MRAS^{CC} estimators using direct torque control. *Automatika.* 2013;54(3):329–336.
- [14] Sun X, Li T, Zhu Z, et al. Speed sensorless model predictive current control based on finite position set for PMSM drives. *IEEE Trans Transp Electrification.* 2021;7(4):2743–2752.
- [15] Heras Cervantes M, Tellez Anguiano AdC, Anzurez Marin J. et al. Real-time simulation of a Luenberger observer applied to DC-DC converters. *IEEE Latin Am Trans.* 2018;16(3):981–986.
- [16] Rigatos GG. Particle and kalman filtering for state estimation and control of DC motors. *ISA Trans.* 2009;48(1):62–72.
- [17] Aydogmus O, Talu MF. Comparison of extended kalman and particle filter-based sensorless speed control. *IEEE Trans Instrum Meas.* 2012;61(2):402–410.
- [18] Terzic B, Jadric M. Design and implementation of the extended kalman filter for the speed and rotor position estimation of brushless DC motor. *IEEE Trans Ind Electron.* 2001;48(6):1065–1073.
- [19] Boztas G, Aydogmus O. Implementation of sensorless speed control of synchronous reluctance motor using extended Kalman filter. *Eng Sci Technol Int J.* 2021: 1–7. doi:10.1016/j.jestch.2021.09.012.
- [20] Kung Y-S, Thanh NP, Wang M-S. Design and simulation of a sensorless permanent magnet synchronous motor drive with microprocessor-based PI controller and dedicated hardware EKF estimator. *Appl Math Model.* 2015;39(19):5816–5827.
- [21] Aydogmus Z, Aydogmus O. A comparison of artificial neural network and extended kalman filter based sensorless speed estimation. *Measurement.* 2015;63:152–158.
- [22] Lin F-J, Hung Y-C, Chen J-M, et al. Sensorless inverter-fed compressor drive system using back-emf estimator with PIDNN torque observer. *Asian J Control.* 2014;16(4):1042–1056.
- [23] Cao Y, Wang J, Shen W. High performance PMSM self-tuning speed control system with a low order adaptive instantaneous speed estimator using a low cost incremental encoder. *Asian J Control.* 2020;23(4):1870–1884.
- [24] Senthil Kumar N, Sadasivam V, Muruganandam M. A low-cost four-quadrant chopper-fed embedded DC drive using fuzzy controller. *Electr Power Compon Syst.* 2007;35(8):907–920.
- [25] Sreeram K. Design of fuzzy logic controller for speed control of sensorless BLDC motor drive. 2018 International Conference on Control, Power, Communication and Computing Technologies (ICCPCT), pp. 18–24, 2018.
- [26] Rao JS., Kumar GR, Sekhar OC. Sensorless speed control of brushless DC motor using fuzzy controller. 2016 International Conference on Electrical, Electronics, and Optimization Techniques (ICEEOT), pp. 4082–4085, 2016.
- [27] Wen J-S, Wang C-H, Chang Y-D, et al. Intelligent control of high-speed sensorless brushless DC motor for intelligent automobiles. 2008 IEEE International Conference on Systems, Man and Cybernetics, pp.3394–3398, 2008.
- [28] Boulghasoul Z, Kandoussi Z, Elbacha A, et al. Fuzzy improvement on Luenberger observer base induction motor parameters estimation for high performances sensorless drive. *J Electr Eng Technol.* 2020;15:2179–2197.
- [29] Virkar VS, Karvekar SS. Luenberger observer based sensorless speed control of induction motor with fuzzy tuned PIN controller. 2019 International Conference on Communication and Electronics Systems (ICCES), pp.503–508, 2019.
- [30] Al-Maliki AY, Iqbal K. FLC-based PID controller tuning for sensorless speed control of DC motor. 2018 IEEE International Conference on Industrial Technology (ICIT), pp.169–174, 2018 .
- [31] Kothari DP, Nagrath IJ. *Electric machine.* 4th ed. New Delhi: Tata McGraw Hill; 2010.

Appendix. Motor, load and controller parameter

$$\begin{aligned}
 V_{armature} &= 240 \text{ V}, V_{field} = 300 \text{ V}, \\
 R_a &= 2.581 \Omega, L_a = 0.028 \text{ H}, \\
 L_{af} &= 0.9483 \text{ H}, J = 0.02215 \text{ kg m}^2, \\
 D &= 0.002953 \text{ Nms}, T_f = 0.5161 \text{ Nm}, \\
 m &= 5 \text{ kg}, L = 0.05 \text{ m}, g = 9.81 \text{ m/s}^2, \\
 T_s &= 10^{-4} \text{ s}, k_{ps} = 10, k_{is} = 0.5, \\
 k_{pc} &= 100, k_{ic} = 10, e = [-1, 1], \Delta e = [-2, 2]
 \end{aligned}$$